



Cite this: *Sustainable Energy Fuels*,
2024, 8, 5504

Cycloalkane-rich sustainable aviation fuel production *via* hydrotreating lignocellulosic biomass-derived catalytic fast pyrolysis oils†

Xiaolin Chen,^{ID} Kellene A. Orton, Calvin Mukarakate,^{ID} Katherine Gaston,^{ID}
Gina M. Fioroni, Robert L. McCormick,^{ID} Michael B. Griffin^{ID} and Kristiina Iisa^{ID}*

Sustainable aviation fuel (SAF) produced from lignocellulosic biomass is emerging as an ideal alternative to conventional jet fuel for aviation sector decarbonization. Catalytic fast pyrolysis (CFP) can convert lignocellulosic biomass into relatively stable bio-oil that can be selectively transformed to various transportation fuels through hydroprocessing under conditions of different severities. In this contribution, two CFP oils produced from pine-based feedstocks over different types of catalysts (*i.e.*, ZSM-5 and Pt/TiO₂ catalysts) were hydrotreated at 125 bar in a non-isothermal process with a maximum temperature of 385 °C over a sulfided NiMo/Al₂O₃ catalyst to produce SAF with high cycloalkane concentrations of 89–92 wt%. Cycloalkanes are an important component of jet fuel with advantageous fuel properties, such as high energy density, low sooting, and potential for replacing aromatic hydrocarbons to provide good seal swelling properties. The hydrotreating process successfully converted 91–92% of the biogenic carbon in the CFP oil intermediates to liquid-phase hydrotreated products. Through distillation, 39–40 wt% of the hydrotreated oils were collected in the jet-fuel range as SAF fractions. The rest of the hydrotreated product could be valorized as fuels (*e.g.*, diesel) or chemicals. The SAF fractions with oxygen contents below the detection limit (<0.01 wt%) met ASTM D7566 finished fuel blend and D4054 Tier 1 specifications with respect to density, lower heating value (LHV), volatility, flash point, and freeze point. These results indicate hydrotreating lignocellulosic biomass-derived CFP oil as a promising pathway to produce high-quality SAF rich in cycloalkanes. Continued research is required to increase the SAF yield by process improvements, such as increased CFP oil yields, and an enhanced production of SAF-range molecules *via e.g.*, cracking of high-molecular weight compounds either during CFP or hydrotreating, as well as evaluation of a broader range of jet fuel properties and performance requirements.

Received 19th August 2024
Accepted 17th October 2024

DOI: 10.1039/d4se01151a

rsc.li/sustainable-energy

1. Introduction

Commercial aviation was responsible for 10% of total U.S. transportation carbon emissions in 2020.¹ To decarbonize the global aviation sector, the International Air Transport Association (IATA) set a target of “Fly Net Zero” by 2050 in its 77th Annual Meeting in 2021.² Similarly in 2022, the International Civil Aviation Organization (ICAO) Member States adopted a global goal of net-zero carbon emissions by 2050 for international airlines.³ To achieve the carbon net-zero goal for aviation, accelerating the production and deployment of sustainable aviation fuel (SAF) is required. In 2023, a Grand Challenge issued by the U.S. Departments of Transportation, Energy, and Agriculture set a goal of 3 billion gallons of SAF production per year by 2030 and 35 billion gallons of SAF to meet commercial

jet fuel demand by 2050 in accordance with the goals set by IATA and ICAO. To date, over 95% of the SAF flights have been powered by hydrotreated esters and fatty acids (HEFA) or synthetic paraffinic kerosene (SPK) produced from fats, oils, and greases (FOG) blended at 50 vol% in conventional jet fuel.^{4,5} To avoid competition with food and feed production, the availability of non-food lipids is limited and corresponds to 1.7 billion gallons per year of HEFA production in the U.S., which can't meet the demand for SAF.⁶ It is urgent to supplement FOG with an alternative non-food biomass feedstock for SAF production and thus meet the rapidly growing SAF demand and at the same time avoid the direct competition with feed/food resources.⁷ Woody biomass is an abundant feedstock with 144 million dry short tons of forest and wood resources currently used for energy and coproducts per year in the US.⁸ The near-term and mature-market potentials from forest land resources are estimated to be 31 and 63 million dry short tons per year, respectively; in addition, there is a mature-market potential of 34–103 million dry short tons per year of woody energy crops. In contrast, the near-term potential waste and byproducts for FOG

National Renewable Energy Laboratory, Golden, CO, USA. E-mail: kristiina.iisa@nrel.gov

† Electronic supplementary information (ESI) available. See DOI: <https://doi.org/10.1039/d4se01151a>



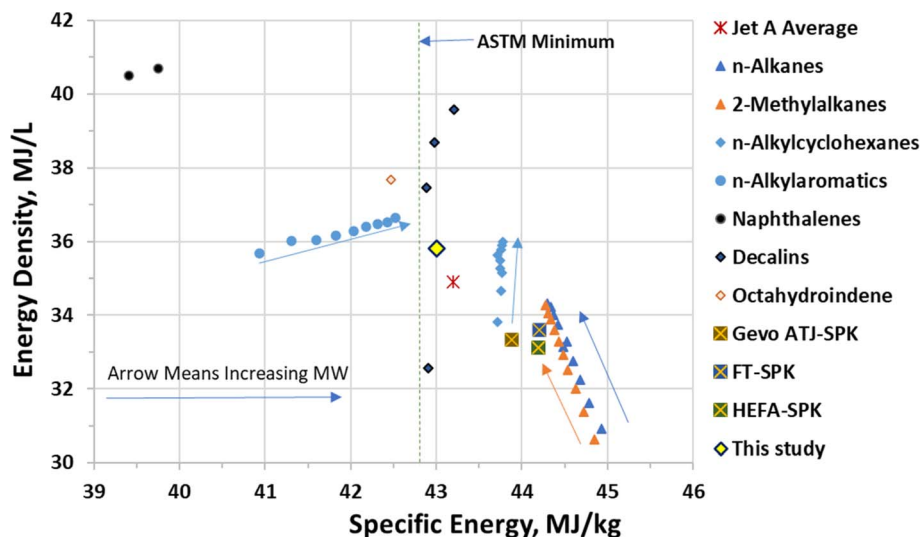


Fig. 1 Energy density vs. specific energy (lower heating value, LHV) for selected compound types, jet A average, and selected Synthetic Paraffinic Kerosenes (SPK).

is only 3 million dry short tons per year with a mature-market potential of 28 million dry short tons per year of intermediate oilseeds. Therefore, lignocellulosic biomass is regarded as a promising key solution to replace fossil fuels to power the transportation sector and reduce carbon dioxide emissions.^{9–11}

Catalytic fast pyrolysis (CFP) is a promising technology to convert lignocellulosic biomass into stable low-oxygen bio-oil.¹² Solid acid catalysts, such as zeolites (*e.g.*, ZSM-5) and bifunctional catalysts with both hydrogenation and acidic functionalities, such as noble metals (*e.g.*, Pt, Pd, Ru) supported on reducible oxides (*e.g.*, TiO₂, ZrO₂), have been widely used for biomass pyrolysis vapor deoxygenation during CFP.¹³ Zeolites are well-known industrial catalysts suitable for fluidized bed and riser reactors due to their good attrition resistance properties.^{14–16} Among common zeolite catalysts (*e.g.*, mordenite, beta, ZSM-5), ZSM-5 is the most effective for aromatic hydrocarbon production and coke reduction during CFP.¹⁷ ZSM-5 can remove oxygen *via* various reactions: decarbonylation, decarboxylation, dehydration, cracking, and coupling into light alkenes and aromatic hydrocarbons.^{13,18,19} Bifunctional catalysts (*e.g.*, Pt/TiO₂) with co-fed H₂ are often utilized to remove oxygen from bio-oil by forming water *via* hydrodeoxygenation and direct deoxygenation and usually result in higher CFP oil yields (*vs.* zeolite catalysts) attributed to the hydrogenation of coke precursors in the presence of H₂.^{13,18,20,21} However, bifunctional catalysts often require fixed bed reactors since they are expensive and the attrition in fluidized beds results in a high catalyst replacement rate and thus high operating costs.^{11,21}

The residual oxygen in CFP oil can be further removed in a single-stage hydrotreating process through hydrodeoxygenation reactions and the products can be fractionated into gasoline, SAF, diesel, and marine fuel through distillation.^{13,22} Conventional petroleum-derived jet fuels consist of molecules with carbon numbers of C₉–C₁₈ boiling in the temperature range of 125–290 °C. Typically, jet fuels are

composed of 13–26 wt% of linear alkanes, 19–37 wt% of isoalkanes, 22–47 wt% of cycloalkanes, and 14–21 wt% of aromatics.⁶ Cycloalkanes are a key component of jet fuels due to their desirable fuel properties (*e.g.*, high energy density, low freeze point, and high density). While linear alkanes have the highest cetane number among hydrocarbons of the same carbon number, they have low energy densities (Fig. 1) and high freeze point relative to standard aviation fuel specifications. Compared to linear alkanes, isoalkanes exhibit lower freeze points. While aromatics provide the majority of the volume swell for nitrile rubber O-rings and seals, they have low specific energy (energy per unit mass – see *n*-alkylaromatics and naphthalenes in Fig. 1), and are the primary contributor to particulate matter emissions.^{6,23,24} Faulhaber and colleagues investigated nitrile rubber swelling for a broad range of individual cycloalkanes and aromatics. They showed that much higher cycloalkane concentrations are required relative to aromatics for the same level of swell. Among the cycloalkanes, they found cyclohexane and both *cis* and *trans* decalin to have the highest swelling effect.²⁴ Bicycloalkanes such as decalins have much higher energy density (MJ L^{−1}) than conventional jet fuels, while monocyclic alkanes, *e.g.*, cyclohexanes have significantly higher specific energy (MJ kg^{−1}) (Fig. 1).²³ Monocyclic and bicyclic alkanes offer a potential replacement of aromatics for seal swelling capabilities, can have high specific energy, and they have low sooting indices.^{24,25} So far, HEFA-SPK and other approved SAF pathways such as Fischer–Tropsch (FT), Alcohol-to-Jet (ATJ) SPK's mainly contain linear and isoalkanes and can only be used at up to 50 vol% in conventional jet fuel.^{26–29} Consequently, a vision for SAF that could be used at up to 100% as a drop-in fuel is to reduce or eliminate aromatic content and increase cycloalkane content.

CFP oils contain phenols, higher hydroxyaromatics such as indenols and naphthols, aromatic hydrocarbons, carbonyls (ketones and aldehydes), furans, and anhydro sugars.^{13,18,30}



Through hydrotreating, phenols, cyclic ketones (e.g., cyclopentenones and cyclopentanones), and aromatic hydrocarbons could be hydrodeoxygenated and hydrogenated into cycloalkanes.^{9,11} Studies of hydrotreating CFP oil at high temperatures (390–400 °C) over sulfided NiMo and CoMo catalysts have shown high fractions of aromatic hydrocarbons along with some cycloalkanes in the hydrotreated product.^{21,31} A previous study showed the production of cycloalkanes could be significantly enhanced by hydrotreating CFP oil in a non-isothermal process with a maximum temperature of 385 °C that favored the hydrogenation of aromatic hydrocarbons.⁹ As a result, 78 wt% of the diesel fraction was constituted of cycloalkanes. The production of SAF from CFP oils produced over ZSM-5 catalyst under similar conditions contained 71–72% cycloalkanes.³²

The objective of this contribution is to showcase the production of cycloalkane-rich SAF fractions with satisfactory fuel properties fulfilling selected Tier 1 aviation fuel standard specifications (ASTM D7566 finished fuel blend properties and D4054 Tier 1 properties) through hydrotreating two types of CFP oils, produced over traditional ZSM-5 and bifunctional Pt/TiO₂ catalysts. In addition, this contribution provides detailed experimental information of the production and properties of the CFP oils, hydrotreated oils, and SAF fractions to enrich the previous work, which modelled SAF properties based on GC × GC analysis.³³

2. Experimental

2.1 Materials

The biomass feedstocks were pine-based woody biomass supplied by Idaho National Laboratory. The elemental composition of the biomass feedstocks is given in Table S1 in the ESI.† The Pt/TiO₂ catalyst for CFP contained 0.5 wt% Pt, and it was prepared by strong electrostatic adsorption and supported on 0.5 mm diameter near-spherical particles of 85% anatase/15% rutile (TiO₂) provided by Johnson Matthey.²¹ The zeolite catalyst for CFP was fresh ZSM-5 GC-4 purchased from Equilibrium Catalyst, Inc., a commercial supplier of catalyst for FCC units in oil refineries. The ratio of SiO₂ to Al₂O₃ (mol mol⁻¹) was approximately 30. The average particle size was 60 μm. The zeolite catalyst was cyclone-classified to remove fines (<20 μm) before loading into the reactor. The catalyst used for hydrotreating experiments was NiMo on alumina support (NiMo/Al₂O₃) provided by Johnson Matthey and crushed to an approximate particle size of 0.5 mm. The NiMo/Al₂O₃ catalyst contained 3.7 wt% of Ni and 11.5 wt% of Mo, and it had a BET surface area of 170 m² g⁻¹, a pore volume of 0.4 cm³ g⁻¹, and a median pore diameter of 97 Å determined by N₂ physisorption.⁹ Green Silicon Carbide (SiC), 24 grit with an average particle size of 686 μm, was purchased from Panadyne, Inc.

2.2 CFP experiments

The CFP oils were produced in two different facilities at the National Renewable Energy Laboratory (NREL). The Pt/TiO₂-CFP oil was produced with co-fed H₂ at atmospheric pressure in

Table 1 CFP experiments

Catalyst	Pt/TiO ₂	ZSM-5
Biomass feedstock	Loblolly pine and/or pine forest residues	Loblolly pine
Biomass feed rate, kg h ⁻¹	0.15	10
Pyrolysis temperature, °C	500–525	500
Upgrading reactor type	Fixed bed	Riser
Upgrading temperature, °C	400	550
Gas atmosphere	85% H ₂ /15% N ₂	N ₂

an *ex situ* bench-scale unit in the 2-inch Fluidized Bed Reactor (2FBR) system, which consisted of a 5 cm inner diameter fluidized bed pyrolyzer and a fixed bed catalytic upgrading reactor.^{20,21} The ZSM-5-CFP oil was produced in an *ex situ* pilot-scale system in the Thermal and Catalytic Process Development Unit (TCPDU), which consisted of an entrained-flow pyrolyzer and a circulating riser catalytic upgrader.³⁴ The riser with a 4-inch diameter was heated by external electric heaters. The pyrolysis vapors entered the riser from the bottom and mixed with regenerated catalyst and carrier gas in a mixing cup. The catalyst particles were entrained in the pyrolysis vapors, and they both traveled upwards through the riser reactor. The catalyst particles were then separated in a cyclone and recycled through a steam stripper and a regenerator, in which coke was burnt off. The feedstocks, and conditions of the CFP experiments are summarized in Table 1.

2.3 Hydrotreating experiments

The CFP oils were hydrotreated over the sulfided NiMo/Al₂O₃ catalyst in a continuous trickle-bed hydrotreater system at NREL.⁹ The liquid feed (*i.e.*, CFP oil) was introduced through a 500 mL ISCO syringe pump, and the gas feed (*i.e.*, H₂ with 150 ppm H₂S) was fed from a customized cylinder and compressed. The combination of the liquid feed and the gas feed were injected to the trickle-bed reactor through a syringe tip and flowed through the catalyst bed placed in the inner tube of a tube-in-tube heat exchanger. The reactor (122 cm tall with a 0.84 cm inner diameter) contained a thermocouple well (0.32 cm outside diameter) with six thermocouples along the centerline. The reactor was placed in a four-zone electric 2000 W furnace and heated by a gas (*i.e.*, air) flowing in the outer tube. A heat transfer working fluid (air) was chosen since it can both heat and reduce the temperature in case of a run-away reaction. The products were condensed in two 150 mL collection vessels chilled to 5 °C, alternated approximately every 12 h. The collected hydrotreated products were separated into organic and aqueous phases, which were both weighed and analyzed for composition. The exit gas flow was measured by a Coriolis flow meter and its composition was measured by a micro-GC and NDIR analyzer. Mass and carbon balances were calculated for each 12 h period. At the beginning of each experiment, the catalyst was presulfided with a mixture of 35 wt% di-*tert*-butyl disulfide and 65 wt% decane, where the temperature was first held at 150 °C for 2 h, then ramped to the reaction temperature, and held for 4 h, all at the reaction pressure. 150 ppm H₂S was



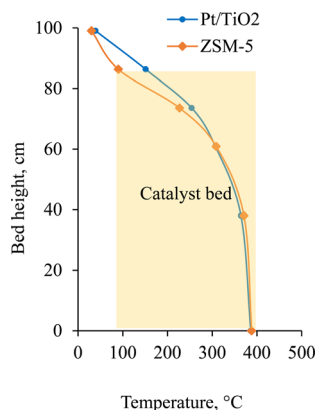


Fig. 2 Hydrotreater temperature profiles.

included in the H_2 gas to maintain the catalyst activated during hydrotreating. The liquid feed was started after presulfidation.

The temperature profile of the catalyst bed included an initial low-temperature transition zone followed by a high-temperature isothermal zone from the top to the bottom of the reactor (Fig. 2). For hydrotreating the CFP oils, the total weight hourly space velocities (WHSV) were $0.11\text{--}0.12\text{ h}^{-1}$ with 22 g of catalyst for the Pt/TiO₂-CFP oil (density 1.02 g mL^{-1}) and 28.2 g of catalyst for the ZSM-5-CFP oil (density 1.19 g mL^{-1}). In both cases, 12.5 g of catalyst was placed in the near-isothermal zone, topped by the rest of the catalyst, which was diluted with SiC to keep exotherms around 1°C . More catalyst was included for the ZSM-5-CFP oil due to its higher density and higher oxygen content (Table 1). For the Pt/TiO₂-CFP oil, the catalyst bed started at 150°C , for the ZSM-5-CFP oil, it started at 90°C . The hydrotreating pressure was 125 bar (1800 psi). 2.5 mL h^{-1} of the CFP oil were fed with 200 mL min^{-1} of H_2 with 150 ppm H_2S over the catalyst bed. The hydrotreating of the Pt/TiO₂-CFP oil and the ZSM-5-CFP oil was continued for 70 h and 50 h, respectively, without operational problems (e.g., system plugging).

2.4 Liquid characterization

The CFP oils were analyzed for CHN on a LECO 628 series TruSpec® Analyzer, for ash by thermogravimetric analysis (TGA) on LECO TGA 701 TruSpec® Analyzer, for sulfur by inductively coupled plasma-optical emission spectroscopy (ICP-OES) on an Agilent 5100, and for water by Karl-Fischer titration (NREL/TP-5100-80968, ASTM D7544). The carboxylic acid number (CAN) of the CFP oil was determined by modified ASTM D664.³⁵ The hydrotreated oils and the SAF fractions were analyzed for CHNS, and water by Karl Fisher titration at Huffman-Hazen Laboratories (Golden, CO).¹⁹ Direct oxygen was measured on an Elementar VEL Cube equipped with NDIR detectors. The density was measured at 15°C on Mettler Toledo D4 (ASTM D4052).

The CFP oils were analyzed by ^{13}C nuclear magnetic resonance (NMR),^{21,36,37} gas chromatography coupled to mass spectrometry and flame ionization detection (GC-MS-FID),²¹ gel permeation chromatography (GPC),¹⁹ and simulated distillation by TGA (TGA-SimDist).²⁰ The hydrotreated oils and SAF

fractions were analyzed by two-dimensional gas chromatography with simultaneous time-of-flight mass spectrometry and flame ionization detection (GC \times GC-TOFMS-FID).⁹ The hydrotreated oils and SAF fractions were analyzed by simulated distillation (ASTM D2887). The diesel fractions were analyzed for compound groups by gas chromatography with vacuum ultraviolet spectroscopy (GC-VUV).⁹ More details of the analytical methods are included in the ESI.†

The hydrotreated oils were fractionated into different fuel cuts using a B&R micro spinning band distillation unit equipped with a metal band with fourteen theoretical plates. The light fraction boiling below 70°C was separated by atmospheric distillation and the fractions with higher boiling points were separated by vacuum distillation at 658 Pa (5 Torr). The fractions with atmospheric equivalent temperatures (AETs) below 145°C were classified as the gasoline range, and those with AETs of $145\text{--}245^\circ\text{C}$ were designated as the SAF range.¹³ The fuel properties of the SAF fractions were analyzed including density at 15°C (ASTM D7042), heating values (ASTM D240), freeze point (ASTM D5972), flash point (ASTM D6450), and volatility by simulated distillation (ASTM D2887 D86 correlation).

3. Results and discussion

3.1 CFP oils

Two CFP oils were compared here: one produced over a bifunctional metal/acid Pt/TiO₂ catalyst and one over a solid-acid ZSM-5 zeolite. Both catalysts deoxygenate pyrolysis vapors though the mechanisms differ. Pt/TiO₂ is a hydrodeoxygenation catalyst and hydrogen was co-fed into the pyrolysis reactor for this catalyst. Because of this functionality, Pt/TiO₂ gives higher CFP oil yields than ZSM-5 does, due to decreased coke formation and retention of longer side chains in lignin-derived compounds.^{13,21} CFP oils produced over Pt/TiO₂ have a high abundance of phenols without additional oxygen functional groups and cyclopentenones. ZSM-5 oils, in contrast, may contain higher concentration of compounds with multiple oxygen functionalities, such as hydroxyacetaldehyde and hydroxypropanone, in addition to fully deoxygenated aromatic hydrocarbons. The ZSM-5 catalysts also produce multi-ring fused aromatic compounds, such as higher hydroxy aromatics

Table 2 Composition of CFP oils

CFP oil	Pt/TiO ₂	ZSM-5
C, wt% daf	76.42 ± 0.04	74.67 ± 0.41
H, wt% daf	7.78 ± 0.13	6.92 ± 0.06
N, wt% daf	0.19 ± 0.02	0.19 ± 0.03
O, wt% daf (by difference)	15.61	18.22
Ash, wt%	0.27 ± 0.31	1.21 ± 0.07
H ₂ O, wt%	2.83 ± 0.03	10.84 ± 0.17
H : C, mol/mol (daf)	1.2	1.1
H : C _{eff} ^a , mol/mol	0.92	0.75
Density, g mL ⁻¹	1.020	1.185
CAN, mg _{KOH} g ⁻¹	39.0 ± 0.7	21.1 ± 0.4

^a (H-2 \times O)/C.



(e.g., indenols and naphthols) and aromatic hydrocarbons (e.g., indenes and naphthalenes), which are not present in appreciable amounts in non-catalytic pyrolysis oils and are not formed in lower quantities over Pt/TiO₂.

The elemental compositions of the CFP oils are given in Table 2. The Pt/TiO₂-CFP oil contained 16 wt% oxygen, and the ZSM-5-CFP oil contained 18 wt% oxygen on dry ash free (daf) basis. Compared to the Pt/TiO₂-CFP oil, the ZSM-5-CFP oil had higher water and ash contents, and a lower effective hydrogen to carbon ratio ($H : C_{eff}$).

The ¹³C NMR analysis results of CFP oils are given in Fig. 3. The aromatic bonds including aromatic C–C, C–H, C–O were abundant in both CFP oils, accounting for 58 and 72% of the total carbon bonds in the Pt/TiO₂-CFP oil and the ZSM-5-CFP oil, respectively. This indicates a high potential for cycloalkanes formation *via* aromatic ring hydrogenation and deoxygenation during hydrotreating of these CFP oils. Aromatic C–O bonds constituted 21–28% of the total aromatic carbons, suggesting that the aromatic compounds were mainly phenolics or higher hydroxyaromatics, e.g., naphthols and indenols. It should be noted that C=C, C–C, and C–O bonds in furan rings also show up within the aromatic range in this ¹³C NMR classification, and some of the bonds labelled aromatic may have been in furans or cycloalkenes, e.g., cyclopentenones.³⁶ Methoxy groups were low corresponding to 1–2% of aromatic carbons, indicating efficient demethoxylation in both CFP oils. Aliphatic C–C bonds constituted the next major group (24–36%) and were likely composed of side chains in the hydroxyaromatic compounds. Aliphatic C–C bonds were more abundant in the Pt/TiO₂-CFP oil (36% *vs.* 24% in the ZSM-5-CFP oil) in accordance with the retention of longer side chains by the hydrodeoxygenation catalyst (*i.e.*, Pt/TiO₂).²¹ Aliphatic oxygens including C=O and aliphatic C–O bonds in acids, ketones, aldehydes, and anhydro sugars were quite low in both CFP oils, with C=O bonds constituting 4% in the Pt/TiO₂-CFP oil and 1% in the ZSM-5 CFP oil, and aliphatic C–O bonds accounting only for 0.5–1.3%. This suggests that typical carbohydrate-derived,

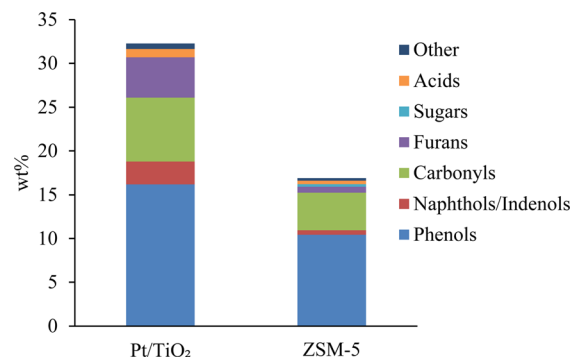


Fig. 4 Major compound groups identified by GC-MS for CFP oils.

non-upgraded pyrolysis compounds were present at low concentrations in both CFP oils.

Volatile and semi-volatile compounds were identified by GC-MS analysis (Fig. 4). 31 wt% of the Pt/TiO₂-CFP oil and 17 wt% of the ZSM-5-CFP oil were GC-MS detectable compounds. The lower GC-MS detectable fraction in the ZSM-5-CFP oil indicates a higher fraction of high-molecular weight compounds with high boiling points in the ZSM-5-CFP oil. This was confirmed by GPC results (Fig. 5) and TGA-SimDist results (Fig. S2†). The ZSM-5-CFP oil also contained a higher amount of very low-molecular weight material (*vs.* Pt/TiO₂-CFP oil) (Fig. 5), which includes water (Table 2) and acetic acid and hydroxyacetaldehyde detected by GC-MS (Table S2†). The most abundant compound groups in both CFP oils were phenols and carbonyls (*i.e.*, ketones and aldehydes), consistent with the ¹³C NMR analysis. The Pt/TiO₂-CFP oil also had higher contents of furans than the ZSM-5-CFP oil did (Fig. 4). The phenols included methoxyphenols (Fig. S1a†), detected at a higher concentration in the Pt/TiO₂-CFP oil than in the ZSM-5 oil, in agreement with the ¹³C NMR analysis. Carbonyl and acid concentrations were higher in the Pt/TiO₂-CFP oil (8 wt% *vs.* 4 wt% in the ZSM-5-CFP oil) as suggested by the fractions of C=O bonds by ¹³C NMR analysis. The carbonyls in both CFP oils consisted mainly of cyclic ketones (*i.e.*, cyclopentenones and cyclopentanones) (Fig. S1b†), which may also form cycloalkanes during hydrotreating. There were additional differences within the compound classes between the two CFP oils by GC-MS

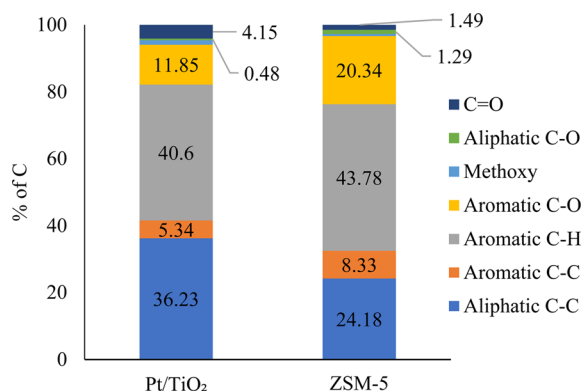


Fig. 3 ¹³C NMR analysis results of CFP oils. The peak integration regions for functional groups are aliphatic C–C (0–55.2 ppm), methoxy (55.2–60.8 ppm), aliphatic C–O (60.8–95.8 ppm), aromatic C–H (95.8–134 ppm), aromatic C–C (134–142 ppm), aromatic C–O (142–166.5 ppm), carbonyl (166.5–225 ppm).³⁷

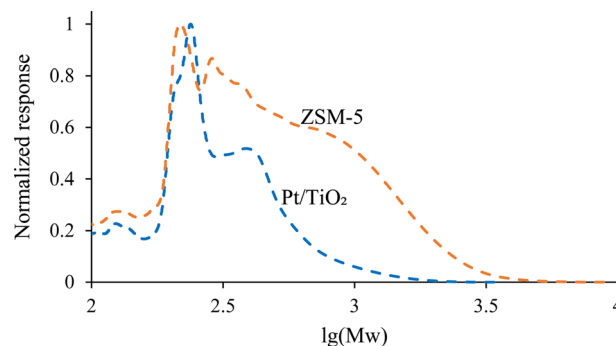


Fig. 5 GPC analysis of CFP oils. The responses have been normalized by setting the highest response to 1. The molecular weights are not absolute but relative to the standards used.



Table 3 Mass and carbon balances for hydrotreating CFP oils and elemental compositions of the hydrotreated oils^a. The mass yields are on dry ashfree (daf) CFP oil basis

Feed	Pt/TiO ₂ -CFP oil	ZSM-5-CFP oil
Oil, g/g daf oil × 100%	80.5	79.7
Aqueous, g/g daf oil × 100%	20.7	21.2
Gas, g/g daf oil × 100%	7.1	7.8
H ₂ consumption, g/g daf oil × 100%	7.8	9.2
Oil, g C/g C in oil × 100%	92.1	91.5
Gas, g C/g C in oil × 100%	7.8	8.5
C, wt%	85.8	86.0
H, wt%	13.8	13.9
O, wt% (by difference)	0.3	0.05
N, wt%	<0.01	<0.01
S, wt%	<0.01	<0.01
H : C, mol : mol	1.94	1.94
Density, g mL ⁻¹	0.79	0.80

^a The balances are normalized. Actual mass balance closures were 98–105% based on CFP oil feed and hydrogen consumption, and actual carbon balance closures were 95–103%.

analysis, for example, the Pt/TiO₂-CFP oil had a higher concentration of methoxyphenols, and the ZSM-5-CFP oil contained more benzenediols (Fig. S1a†). Within carbonyls, the ZSM-5-CFP oil contained aldehydes while they were not detected in the Pt/TiO₂-CFP oil (Fig. S1b†). Carboxylic acids accounted for 0.9 wt% and 0.4 wt% in the Pt/TiO₂-CFP oil and the ZSM-5-CFP oil, respectively (Fig. 4), corresponding to CANs of 39 and 21 (Table 2). The acid numbers are reduced by factors of 2–3, compared to non-catalytic pyrolysis oil values (76) from similar conditions.³¹

Overall based on the analyses, the CFP oils had high contents of phenols and higher hydroxyaromatics with cyclic ketones as the next most abundant compound group within the volatile and semi-volatile GC-MS-detectable fraction. However, over half of the CFP oils was non-GC-MS detectable with boiling points above 300 °C, and this material also appeared to consist largely of hydroxyaromatics. The aromatic and cyclic structures in the CFP oils show great potential for cycloalkane formation during hydrotreating.

3.2 CFP oil hydrotreating

The CFP oils were hydrotreated over sulfided NiMo/Al₂O₃ in a bench-scale trickle-bed hydrotreater system. The reactor consisted of two zones: a non-isothermal transition zone in which temperature gradually increased from 90/150 °C to the final hydrotreating temperature aimed at hydrogenating aromatic rings, and an isothermal zone (385 °C) aimed at deoxygenation. Compared to isothermal hydrotreating, this two-zone process has been shown to promote hydrogenation of aromatic rings and formation of cycloalkanes.⁹ The normalized hydrotreating mass and carbon balances are given in Table 3. The Pt/TiO₂ and ZSM-5 CFP oils contained a total of 3.1 and 12.3 wt% of water + ash, respectively (Table 2). These compounds do not react during hydrotreating and in order to give a fair comparison, the mass yields and hydrogen

consumption are given on the basis of dry ashfree (daf) CFP oil. On that basis, the mass yields were relatively similar, with the organic phase (oil) yield slightly lower, aqueous phase yield and hydrogen consumption slightly higher for the ZSM-5-CFP oil than for the Pt/TiO₂-CFP oil. These results are all consistent with the higher oxygen and high molecular weight material contents and lower H : C ratio of the ZSM-5-CFP oil. The hydrotreating carbon efficiency of the Pt/TiO₂-CFP oil was slightly higher (92% vs. 91% for the ZSM-5-CFP oil). Negligible water was detected in the hydrotreated oils. The majority of the carbon loss was caused by light gas formation, namely alkanes with carbon numbers of C₁–C₅. The yields of individual gas products are given in Table S3.† The elemental compositions and densities of the two hydrotreated oils were very similar (Table 3). The oxygen content (measured by difference) was decreased to ≤0.3 wt% (wet basis) by hydrotreating, compared to 16–18 wt% (daf basis) in the CFP oils. The nitrogen and sulfur contents were below detection limits (<0.01 wt%). The H : C ratios of the hydrotreated oils were as high as 1.94 (vs. 1.1–1.2 of CFP oils) indicating a high degree of hydrogenation of aromatic rings during the hydrotreating processes.

The bed temperature profiles (Fig. 2) show a higher temperature for the Pt/TiO₂-CFP oil than for the ZSM-5-CFP oil at the top of the hydrotreater bed. This could be attributed to a higher exothermicity for the Pt/TiO₂-CFP oil in this section. The higher organic content (100% – water – ash) of the Pt/TiO₂ would have increased the heat formation in this section. The Pt/TiO₂-CFP oil also contained more of the lower molecular weight material (Fig. 5), which would react at the top zone. The ZSM-5 oil had more water (11 wt% vs. 3 wt%) that needed to be evaporated, which would have cooled the bed with the ZSM-5-CFP oil. All these factors could have contributed to the higher top temperature for the Pt/TiO₂-CFP oil.

A recent study by Rowland *et al.*³⁸ identified the fraction of high-molecular weight material (material with molecular weight >500 Da) as a good predictor for viscosity after accelerated aging at 100 °C. High viscosity after aging can be correlated to polymerization reactions, and hence the fraction of high-molecular weight material may be a good predictor of polymerization reactions and by extension of bed fouling and plugging problems during hydrotreating. No increases in the pressure drop over the bed during hydrotreating was detected with either CFP oil in this study; however, the high fraction of high-molecular weight material in the ZSM-5-CFP oil may suggest a higher polymerization tendency for this oil.

Table 4 Mass yields for fuel range cuts from distillation of the hydrotreated products

Mass yield, wt%	AET, °C	Pt/TiO ₂	ZSM-5
Gasoline	<145	34	36
SAF	145–245	40	39
Diesel	245–300	11	14
Total fuel range	<300	85	89
Residue	>300	12	8
Losses	N/A	3	3



3.3 SAF fractions

The hydrotreated oils were fractionated into fuel cuts in a spinning band distillation unit (Table 4). The SAF fractions constituted 40 wt% and 39 wt% of the hydrotreated oils derived from the Pt/TiO₂-CFP oil and the ZSM-5-CFP oil, respectively. The elemental compositions of the SAF fractions are given in Table 5. The H : C ratios of the SAF fractions were approximately 1.9 indicative of the high degree of hydrogenation achieved during hydrotreating. The oxygen, nitrogen, and sulfur contents were all below the detection limit (<0.01 wt%) indicating effective deoxygenation, desulfurization, and denitrogenation. The LHV and energy densities of the products are very similar to those for average jet A (Fig. 1).

GC × GC-TOFMS-FID analysis results of the SAF fractions are summarized in Fig. 6a. No oxygenates were detected, consistent with the oxygen contents below the detection limit (<0.01 wt%) (Table 5). The SAF fractions mainly consisted of cycloalkanes (92 wt% for the Pt/TiO₂-CFP oil and 89 wt% for the ZSM-5-CFP oil), which are the key components for aviation fuel with desirable fuel properties. The aromatic hydrocarbons were very low (3–4 wt%) in the SAF fractions since most of them were hydrogenated to form cycloalkanes. The composition of the cycloalkane groups for the SAF fractions are given in Fig. 6b. The results show the majority of the cycloalkanes were cyclohexanes (Fig. 6b), which can be formed from phenols and one-ring aromatic hydrocarbons *via* hydrogenation and deoxygenation and *via* hydrogenation. The second major component in the cycloalkane group was two-ring cycloalkanes, which can be formed by hydrogenation and deoxygenation of two-ring

Table 5 Elemental composition and properties of the SAF fractions

	ASTM D7566	ASTM D4054	Pt/TiO ₂	ZSM-5
C, wt%			86.5	86.5
H, wt%			13.8	13.6
N, wt%			<0.01	<0.01
O, wt%			<0.01	<0.01
S, wt%			<0.01	<0.01
H : C, mol : mol			1.92	1.89
Density 15 °C, g cm ⁻³	775–840	730–880	833	834
Freeze point, °C	≤40	<40	≤70	≤70
Flash point, °C	>38	<68	46.6	49.6
LHV, MJ kg ⁻¹	>42.8	—	43.0	43.0
Energy density, MJ L ⁻¹			35.8	35.8
SimDist D86 correlation				
T10, °C	<205	150–205	170	174
T50, °C	—	165–229	189	191
T90, °C	—	190–262	232	224
FBP, °C	<300	<300	257	249
T50–T10, °C	≥15	≥15	19	17
T90–T10, °C	≥40	≥40	62	49

hydroxyaromatics (*i.e.*, naphthols and indenols) or two-ring aromatics. The CFP process involves coupling and cyclization reactions, which produce fused rings.^{18,19} The production of multirings is in particular prominent for the ZSM-5 catalyst, which also showed a low fraction of compounds not identified by GC-MS (Fig. 4) and a high fraction of high-molecular weight compounds (Fig. 5). In addition, the SAF cuts included small fractions of cyclopentanes, which can be formed by hydrodeoxygenation of C₅-ketones (*i.e.*, cyclopentanones and cyclopentenones) and hydrogenation of cyclopentenenes.

Select fuel properties of the SAF fractions were measured and compared with ASTM D7566 (Standard Specification for Aviation Turbine Fuel Containing Synthesized Hydrocarbons) and ASTM D4054 (Standard Practice for Evaluation of New Aviation Turbine Fuels and Fuel Additives) (Table 5). The SAF fractions derived from both CFP oils met the requirements with respect to the measured properties, *i.e.*, density, freeze point, flash point, lower heating value (LHV), and volatility. In particular freeze points are very low, and distillation slope values well above minimum requirements, suggesting that blending up to the currently allowed 50 vol% is possible. To achieve the same elastomer swell at 8% aromatics (minimum requirement in D7566) requires roughly 30% cycloalkane, suggesting that hydrotreated CFP SAF has potential for use as a neat drop-in fuel – although considerable additional research is necessary to validate this idea.²⁴ This indicates forming high fractions (approximately 90 wt%) of cycloalkanes *via* hydrotreating CFP oil can produce SAF with promising fuel properties.

3.4 Gasoline and diesel fractions

The rest of the hydrotreated liquid product could be valorized as fuels and chemicals. In addition to SAF, 34–36 wt% and 11–14 wt% of the hydrotreated products boiled in the gasoline and diesel range, respectively (Table 4). The residues from distillation could be further converted to fuel-range molecules *via*

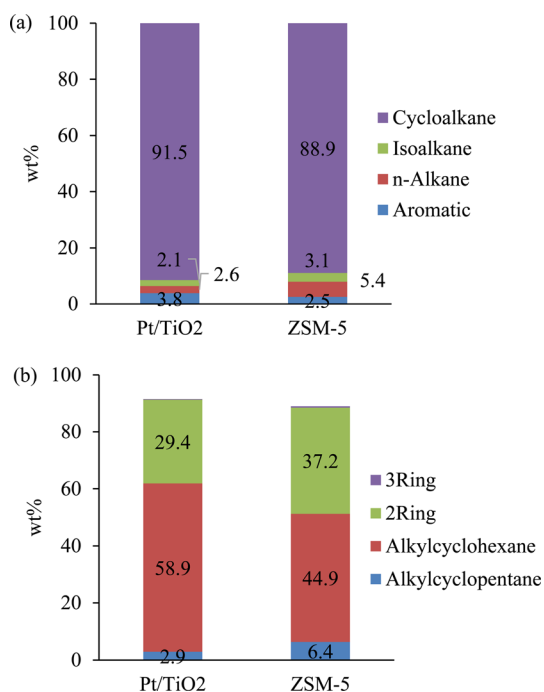
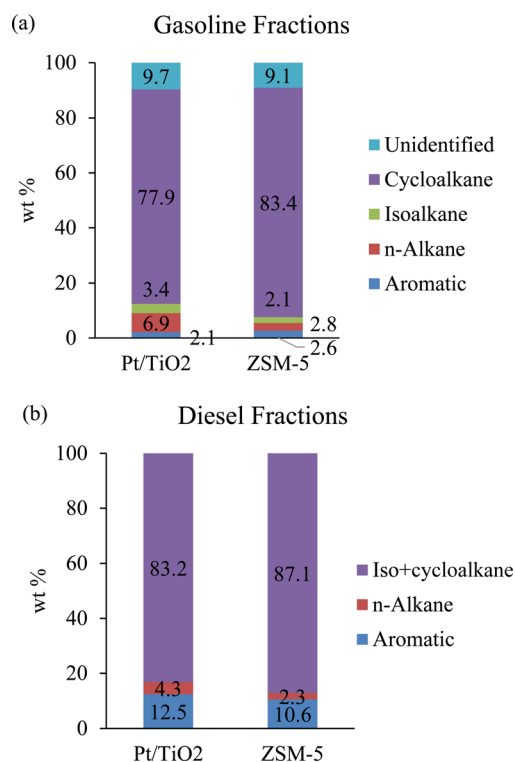


Fig. 6 GC × GC-TOFMS-FID analysis of the SAF fractions. (a) Composition by major compound group; (b) composition within the cycloalkane group.



Table 6 Elemental composition of gasoline and diesel fractions

	Gasoline fractions		Diesel fractions	
	Pt/TiO ₂	ZSM-5	Pt/TiO ₂	ZSM-5
C, wt%	85.4	85.5	87.0	86.9
H, wt%	14.6	14.6	13.4	13.3
N, wt%	<0.01	<0.01	<0.01	<0.01
O, wt%	0.03	<0.01	<0.01	<0.01
S, wt%	<0.01	<0.01	0.01	0.01
H : C, mol : mol	2.06	2.04	1.85	1.84

**Fig. 7** (a) GC-MS-FID analysis of the gasoline fractions and (b) GC-VUV analysis of the diesel fractions.

recycling back to the hydrotreater.³⁹ The elemental compositions of the gasoline and diesel fractions are given in Table 6. The CFP catalyst type had a negligible impact on the elemental composition of the fractions, while the gasoline-range fractions exhibited higher H : C ratios than the diesel fractions did (2.04–2.06 *vs.* 1.84–1.85). The gasoline-range fraction mainly consisted of cycloalkanes by GC-MS-FID analysis (Fig. 7a) with cyclohexane, methylcyclohexane, and ethylcyclohexane the most prominent products (Table S4†). These gasoline-range products could be utilized as solvents or fed to the naphtha reformer to produce aromatic hydrocarbons.

The diesel-range fractions mainly contained iso- and cycloalkanes (83–87 wt%) by GC-VUV analysis (Fig. 7b). Our experience comparing GC-VUV analysis and GC × GC-TOFMS-FID analysis results suggests that the GC-VUV method is not able to correctly differentiate between iso- and cycloalkanes in

hydrotreated CFP oils, and, therefore, we report them together. We assume these to comprise mainly cycloalkanes. This is consistent with previously reported results that the full diesel-range product from a similar two-zone hydrotreating process consisted largely of cycloalkanes (78 wt%).⁹ The diesel fraction in that study exhibited acceptable cetane number and the same could be expected for this diesel-range product.

4. Conclusions

CFP oils produced over Pt/TiO₂ and ZSM-5 catalysts from woody biomass were hydrotreated in a non-isothermal process over sulfided NiMo/Al₂O₃, and this produced SAF fractions that had negligible oxygen content and acceptable LHV, density, freeze point, flash point, and volatility per ASTM D7566 and D4054 specifications. The carbon efficiencies for hydrotreating were 91–92%, and the SAF fractions constituted 39–40% of the hydrotreated organic product. The SAF fractions contained 89–92 wt% cycloalkanes that have been deemed excellent SAF components that are difficult to access *via* most approved SAF pathways. The results indicate CFP followed by hydrotreating can be a complementary pathway to other existing and emerging technologies (such as HEFA, ATJ, and FT) that provides valuable cycloalkanes. In the future, more research efforts are required to enhance the SAF yields from this process by for example increasing the CFP oil yield, developing more effective catalysts, and modifying CFP or hydrotreating processes to improve the cracking of high-molecular weight compounds and coupling of low-molecular weight compounds, and optimizing CFP or hydrotreating conditions to maximize the SAF fraction yield. In addition, it is necessary to determine additional fuel properties (*e.g.*, seal swelling, sooting, and impurity contents, *e.g.*, N, at ppm level) of SAF fractions, test hydrotreating performance in a longer term, scale up the CFP and hydrotreating processes, and explore high-value applications for the non-SAF-range compounds to make the whole process more profitable.

Data availability

The data supporting this article have been included as part of the ESI.†

Conflicts of interest

There are no conflicts to declare.

Acknowledgements

This work was authored in part by the National Renewable Energy Laboratory, operated by Alliance for Sustainable Energy, LLC, for the U.S. Department of Energy (DOE) under Contract No. DE-AC36-08GO28308. Funding provided by U.S. Department of Energy Office of Energy Efficiency and Renewable Energy Bioenergy Technologies Office. The views expressed in the article do not necessarily represent the views of the DOE or the U.S. Government. The U.S. Government retains and the



publisher, by accepting the article for publication, acknowledges that the U.S. Government retains a nonexclusive, paid-up, irrevocable, worldwide license to publish or reproduce the published form of this work, or allow others to do so, for U.S. Government purposes. The authors gratefully acknowledge the experimental contributions by Sean West, Andy Young, Earl Christensen, Jon Luecke, Jennifer Cavaleri, Tim Swanson, Nick Katsiotis, Scott Palmer, and Dr Rick French.

References

- 1 U.S. Environmental Protection Agency (EPA), *Regulations for Greenhouse Gas Emissions from Aircraft*, 2023, available at: <https://www.epa.gov/regulations-emissions-vehicles-and-engines/regulations-greenhouse-gas-emissions-aircraft>.
- 2 International Air Transport Association (IATA), *Net-Zero Carbon Emissions by 2050*, 2021, available at: <https://www.iata.org/en/pressroom/pressroom-archive/2021-releases/2021-10-04-03/>.
- 3 International Civil Aviation Organization (ICAO), *States adopt a net-zero 2050 global aspirational goal for international flight operations*, 2022, available at: <https://unitingaviation.com/news/environment/states-adopt-a-net-zero-2050-global-aspirational-goal-for-international-flight-operations/>.
- 4 U.S. Government Accountability Office (GAO), *Sustainable Aviation Fuel: Agencies Should Track Progress Toward Ambitious Federal Goals*, 2023, available at: <https://www.gao.gov/products/gao-23-105300>.
- 5 E. Cabrera and J. M. M. De Sousa, *Energies*, 2022, **15**, 2440.
- 6 J. Holladay, Z. Abdullah and J. Heyne, *Sustainable Aviation Fuel: Review of Technical Pathways*, 2020, available at: <https://www.energy.gov/eere/bioenergy/articles/sustainable-aviation-fuel-review-technical-pathways-report>.
- 7 N. A. Huq, G. R. Hafenstine, X. Huo, H. Nguyen, S. M. Tiff, D. R. Conklin, D. Stück, J. Stunkel, Z. Yang, J. S. Heyne, M. R. Wiatrowski, Y. Zhang, L. Tao, J. Zhu, C. S. McEnally, E. D. Christensen, C. Hays, K. M. Van Allsburg, K. A. Unocic, H. M. Meyer, Z. Abdullah and D. R. Vardon, *Proc. Natl. Acad. Sci. U. S. A.*, 2021, **118**, e2023008118.
- 8 U.S. Department of Energy (DOE), *2023 Billion-Ton Report: An Assessment of U.S. Renewable Carbon Resources*, 2024, available at: DOI: [10.23720/BT2023/2316165](https://doi.org/10.23720/BT2023/2316165).
- 9 X. Chen, K. A. Orton, C. Mukarakate, L. Tuxworth, M. B. Griffin and K. Iisa, *Energy Adv.*, 2024, **3**, 1121–1131.
- 10 C. Wang, X. Zhang, Q. Liu, Q. Zhang, L. Chen and L. Ma, *Fuel Process. Technol.*, 2020, **208**, 106485.
- 11 M. M. Yung, C. Mukarakate, K. Iisa, A. N. Wilson, M. R. Nimlos, S. E. Habas, A. Dutta, K. A. Unocic, J. A. Schaidle and M. B. Griffin, *Green Chem.*, 2023, **25**, 6809–6822.
- 12 C. J. Wrasman, A. N. Wilson, O. D. Mante, K. Iisa, A. Dutta, M. S. Talmadge, D. C. Dayton, S. Uppili, M. J. Watson, X. Xu, M. B. Griffin, C. Mukarakate, J. A. Schaidle and M. R. Nimlos, *Nat. Catal.*, 2023, **6**, 563–573.
- 13 K. Iisa, C. Mukarakate, R. J. French, F. A. Agblevor, D. M. Santosa, H. Wang, A. N. Wilson, E. Christensen, M. B. Griffin and J. A. Schaidle, *Energy Fuels*, 2023, **37**, 19653–19663.
- 14 S. Bhatia, *Zeolite Catalysis: Principles and Applications*, CRC Press, Boca Raton, Fla, 1990.
- 15 J. E. Naber, K. P. De Jong, W. H. J. Stork, H. P. C. E. Kuipers and M. F. M. Post, in *Studies in Surface Science and Catalysis*, Elsevier, 1994, vol. 84, pp. 2197–2219.
- 16 Z. Nawaz, T. Xiaoping, S. Naveed, Q. Shu and F. Wei, *Pak. J. Sci. Ind. Res.*, 2010, **53**, 169–174.
- 17 J. Jae, G. A. Tompsett, A. J. Foster, K. D. Hammond, S. M. Auerbach, R. F. Lobo and G. W. Huber, *J. Catal.*, 2011, **279**, 257–268.
- 18 A. Eschenbacher, P. Fennell and A. D. Jensen, *Energy Fuels*, 2021, **35**, 18333–18369.
- 19 K. Iisa, R. J. French, K. A. Orton, M. M. Yung, D. K. Johnson, J. Ten Dam, M. J. Watson and M. R. Nimlos, *Energy Fuels*, 2016, **30**, 2144–2157.
- 20 R. J. French, K. Iisa, K. A. Orton, M. B. Griffin, E. Christensen, S. Black, K. Brown, S. E. Palmer, J. A. Schaidle, C. Mukarakate and T. D. Foust, *ACS Sustain. Chem. Eng.*, 2021, **9**, 1235–1245.
- 21 M. B. Griffin, K. Iisa, H. Wang, A. Dutta, K. A. Orton, R. J. French, D. M. Santosa, N. Wilson, E. Christensen, C. Nash, K. M. Van Allsburg, F. G. Baddour, D. A. Ruddy, E. C. D. Tan, H. Cai, C. Mukarakate and J. A. Schaidle, *Energy Environ. Sci.*, 2018, **11**, 2904–2918.
- 22 F. A. Agblevor, D. C. Elliott, D. M. Santosa, M. V. Olarte, S. D. Burton, M. Swita, S. H. Beis, K. Christian and B. Sargent, *Energy Fuels*, 2016, **30**, 7947–7958.
- 23 S. Kosir, J. Heyne and J. Graham, *Fuel*, 2020, **274**, 117832.
- 24 C. Faulhaber, C. Borland, R. Boehm and J. Heyne, *Energy Fuels*, 2023, **37**, 9207–9219.
- 25 D. D. Das, C. S. McEnally, T. A. Kwan, J. B. Zimmerman, W. J. Cannella, C. J. Mueller and L. D. Pfefferle, *Fuel*, 2017, **197**, 445–458.
- 26 U.S. Department of Energy, Office of Energy Efficiency & Renewable Energy, *Alternative Fuels Data Center (AFDC), Sustainable Aviation Fuel*, 2024 available at: https://afdc.energy.gov/fuels/sustainable_aviation_fuel.html.
- 27 A. De Klerk, G. Chauhan, C. Halmenschlager, F. Link, N. Montoya Sánchez, B. Gartley, H. E. M. El-Sayed, R. Sehdev and R. Lehoux, *Energy Sci. Eng.*, 2024, **12**, 394–409.
- 28 M. Główna, J. Wójcik, P. Boberski, T. Białecki, B. Gawron, M. Skolniak and T. Suchocki, *Renewable Energy*, 2024, **220**, 119696.
- 29 A. Uyaroğlu and M. Unaldi, *Eurasia Proc. Sci. Technol. Eng. Math.*, 2023, **23**, 85–92.
- 30 V. Paasikallio, K. Kalogiannis, A. Lappas, J. Lehto and J. Lehtonen, *Energy Technol.*, 2017, **5**, 94–103.
- 31 K. Iisa, R. J. French, K. A. Orton, A. Dutta and J. A. Schaidle, *Fuel*, 2017, **207**, 413–422.
- 32 M. B. Griffin, K. Iisa, A. Dutta, X. Chen, C. J. Wrasman, C. Mukarakate, M. M. Yung, M. R. Nimlos, L. Tuxworth, X. Baucherel, S. M. Rowland and S. E. Habas, *Green Chem.*, 2024, **26**, 9768–9781.



- 33 S. Watanasiri, E. Paulechka, K. Iisa, E. Christensen, C. Muzny and A. Dutta, *Sustainable Energy Fuels*, 2023, **7**, 2413–2427.
- 34 R. M. Baldwin, K. A. Magrini-Bair, M. R. Nimlos, P. Pepiot, B. S. Donohoe, J. E. Hensley and S. D. Phillips, *Appl. Catal., B*, 2012, **115–116**, 320–329.
- 35 E. Christensen, J. Ferrell, M. V. Olarte, A. B. Padmaperuma and T. Lemmon, *Acid Number Determination of Pyrolysis Bio-oils using Potentiometric Titration: Laboratory Analytical Procedure (LAP)*, 2016, available at: <https://www.osti.gov/servlets/purl/1241091/>.
- 36 R. M. Happs, K. Iisa and J. R. Ferrell III, *RSC Adv.*, 2016, **6**, 102665–102670.
- 37 R. Happs, A. Harman-Ware, H. Ben and J. Ferrell III, *Determination of Carbon Functional Groups in Pyrolysis Bio-Oils using ^{13}C NMR: Laboratory Analytical Procedure (LAP)*, 2021, available at, <https://www.nrel.gov/docs/fy22osti/80969.pdf>.
- 38 S. M. Rowland, R. Martinez, C. J. Wrasman, K. Iisa, M. R. Nimlos and M. B. Griffin, *Energy Fuels*, 2024, **38**, 19626–19638.
- 39 H. Wang, P. A. Meyer, D. M. Santosa, C. Zhu, M. V. Olarte, S. B. Jones and A. H. Zacher, *Catal. Today*, 2021, **365**, 357–364.

